MATCH
Communications in Mathematical and in Computer Chemistry

MATCH Commun. Math. Comput. Chem. **95** (2026) 329–346
ISSN: 0340–6253
doi: 10.46793/match.95-2.15725

Reaction – Diffusion Mechanism for a Possible Spatial Pattern Formation

Miljko V. Satarić[a], **Tomas Nemeš**[b,*]

[a]*Serbian Academy of Science and Arts, Brunch in Novi Sad, Nikole Pašića 6, Novi Sad, 21101, Serbia*

[b]*Faculty of Technical Sciences, Trg Dositeja Obradovića 6, Novi Sad, 21102, Serbia*

sataric.miljko@gmail.com, nemes.tomas@uns.ac.rs

(Received June 25, 2025)

Abstract

The coupling between spatial and temporal order in systems of chemically reacting and diffusing components has an important role in some spatially periodic phenomena including the pattern formation. The model considered here represents a nonlinear reaction-diffusion process where an allosteric enzyme is activated by its reaction product and the reaction is inhibited by depletion of substrate component. The special emphasis here is on the possible role of diffusion of reactants in the initiation of symmetry-breaking instabilities under small spatio-temporal perturbation. We analyzed the necessary and sufficient conditions for possible technological scenario for this kind of autocatalysis where the substrate reactant diffuses faster enough than the product activator, thus enabling the possible symmetry-breaking instability yielding the pattern formation.

*Corresponding author.

1 Introduction

Some five decades ago Nobel prize winner, Ilja Prigogine [1,5,6], proposed the concept of dissipative structures as the dynamical bases of nonequilibrium self-organization in biochemical systems. There are at least two type of biochemical instabilities. The first is generated by homogeneous perturbation, where system goes from a homogeneous steady state to another homogeneous state. The second type is provided by space-dependent inhomogeneous perturbation where diffusion acts as an essential factor of symmetry-breaking event. Diffusion can supply a positive contribution to the excess entropy production in the reaction-diffusion system, leading to the stabilization of the steady state. Otherwise, it increases the manifold perturbation compatible with macroscopic evolution equations. If this effect is dominated, the symmetry-breaking instabilities are possible [2]. Alan Turing [4] proposed that under some specific conditions chemical molecules or morphogen cells can react and diffuse in such a manner as to create of heterogeneous spatial patterns of pertaining reactants concentrations. In the case considered here, we are concerned with the model of two chemical species with spatio-temporal $(\vec{r},t)$ concentrations $X(\vec{r},t)$ and $Y(\vec{r},t)$ which obey the respective reaction-diffusion equations:

$$\begin{aligned} \frac{\partial X}{\partial t} &= f(X,Y) + D_x \bigtriangledown^2 X \\ \frac{\partial Y}{\partial t} &= g(X,Y) + D_y \bigtriangledown^2 Y, \end{aligned} \tag{1}$$

where $f(X,Y)$ and $g(X,Y)$ are the reaction kinetics, which should be essentially nonlinear; D_x, D_y are diagonal matrix elements of positive constant coefficients of diffusion; $\bigtriangledown^2$ stands for Laplace operator. The profound Turing's concept is established as follows: If in nonlinear reaction of above type with missing the diffusion of reactants ($D_x = D_y = 0$), reactants $X(\vec{r},t)$ and $Y(\vec{r},t)$ tend to linearly stable steady state, then under some specified conditions, spatially nonhomogeneous patterns can appear in terms of diffusion driven instability if $D_x \neq D_y$. To understand how the Turing patterns appear, it is necessary to examine this problem in the following way: If we have a reaction-diffusion system with two concentrations of reactants, we can first perform a linear stability analysis. It en-

ables us to determine the conditions under which obtained steady state will be robustly stable against homogeneous perturbations, but under the action of inhomogeneous perturbations steady state undergoes the instability. Quantitatively it appears that the reactant specie $X(\vec{r},t)$ called activator must increase the rate of its own production meaning that at steady state, adding more molecules $X(\vec{r},t)$ causes $\partial X/\partial t$ to increase while substrate $Y(\vec{r},t)$ must yield the rate of its own presence in the reaction to decrease (the positive-feedback reaction). A second very necessary condition for Turing pattern formation is that the substrate must diffuse remarkably more rapidly than the activator reactant:

$$\frac{D_x}{D_y} = r \gg 1, \tag{2}$$

where the necessary ratio r is determined in terms of kinetic constants of reaction and by steady state concentrations X_0 and Y_0. This ratio is typically in the range [7]:

$$6 < r < 10. \tag{3}$$

The condition in Eq. (3) indicates why Turing patterns were very difficult to be achieved experimentally. For example, in aqueous solutions practically all small molecules and ions have diffusion coefficients that lie within a narrow factor of two of

$$10^{-9}\,\mathrm{m^2 s^{-1}}. \tag{4}$$

So obtaining a high value of r within the range of Eq. (3) is extremely difficult seeming impossible in typical chemical systems. These patterns remained experimentally unreachable for about 40 years. Eventually, the group of De Kepper [8, 11], using CIMA reaction (chlorite-iodine-malonic acid reaction) produced conspicuous experimental evidence for Turing pattern appearance.

2 An autocatalytic reaction with two reactants

Let us consider the biochemical reaction in which reactant YX. Importantly, the production of X is autocatalytic process. It means that the reaction accelerates as X increases due to the allosteric catalysis. But rapid depleting of substrate Y inhibits farther production of X, so much that the reaction eventually ceases. In that respect the depletion of Y acts as the inhibition of reaction. This is the case of positive-feedback system. Under such circumstances we can simply use a rate law for the allosteric enzyme and write a pair of nonlinear ordinary differential equations of first order mimicking pertaining mechanism as follows:

$$\frac{dX}{dt} = \nu Y \left[\frac{\varepsilon^2 + \left(\frac{X}{K_n}\right)^2}{1 + \left(\frac{X}{K_n}\right)^2} \right] - K_1 X, \tag{5}$$

$$\frac{dY}{dt} = K_2 - \nu Y \left[\frac{\varepsilon^2 + \left(\frac{X}{K_n}\right)^2}{1 + \left(\frac{X}{K_n}\right)^2} \right]. \tag{6}$$

Here Y substrate is supplied by constant rate $K_2 \left[\mathrm{Ms}^{-1}\right]$ and the product X is created by rate $\nu \left[\mathrm{s}^{-1}\right]$ autocatalyzed by feedback activation expressed in terms of the nonlinear Hill function with coefficients $n = 2$

$$\rho = \frac{\varepsilon^2 + x^2}{1 + x^2} \qquad\qquad x = \frac{X}{K_n}. \tag{7}$$

$K_1 \left[\mathrm{s}^{-1}\right]$ is the rate of removal of product X; K_n [M] is Michealis-Menton generalized constant for the interaction of two-subunit enzyme with substrate to bind. It is inversely proportional to the affinity of the enzyme for substrate. The constant ε^2 is the low activity of the enzyme with no product X bound relative to its highly increased activity when its both regulatory sites are saturated by X molecules. It implies that the inequality

$$\varepsilon \ll 1, \tag{8}$$

safely holds. The shape of function ρ in Eq. (7) is shown in Figure 1.

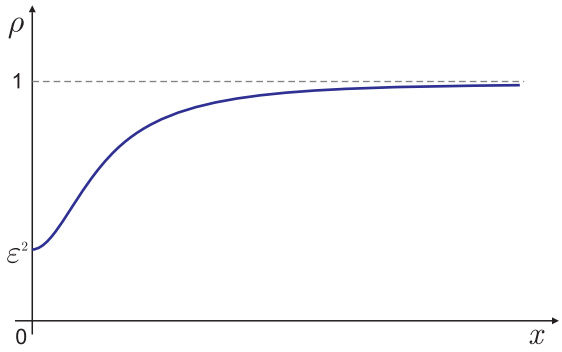

Figure 1. The asymptotic behavior of function ρ from Eq. (7).

It is now plausible to introduce the complete set of dimensionless variables as follows:

$$x = \frac{X}{K_n} \qquad y = \frac{Y}{K_n} \qquad \tau = K_1 t, \tag{9}$$

as well as a new suitable auxiliary variable

$$z = x + y. \tag{10}$$

This transforms Eqs. (5) and (6) in the following shapes

$$\frac{dx}{d\tau} = \mu(z - x)\left(\frac{\varepsilon^2 + x^2}{1 + x^2}\right) - x = f(x, z), \tag{11}$$

$$\frac{dz}{d\tau} = \kappa - x = g(x, z), \tag{12}$$

with new dimensionless kinetic parameters

$$\mu = \frac{\nu}{K_1} \qquad \kappa = \frac{K_2}{K_1 K_n}. \tag{13}$$

The steady-state for this reaction model now reads:

$$\text{for} \qquad \frac{dx}{d\tau} = 0 \qquad \Rightarrow \qquad z_0 = \frac{\kappa}{\rho\mu} + \kappa, \tag{14}$$

$$\text{for} \qquad \frac{dz}{d\tau} = 0 \qquad \Rightarrow \qquad x_0 = \kappa. \tag{15}$$

It could be of interest to plot the corresponding nullclines in the phase plane for Eqs. (11) and (12). For $dx/d\tau = 0$, the x-nullclines reads

$$z = \frac{x(1+x^2)}{\mu(\varepsilon^2 + x^2)} + x. \tag{16}$$

For $dz/d\tau = 0$, the z-nullcline is simply constant

$$x = \kappa. \tag{17}$$

The x-nullcline has two positive extrema at roots of its first derivative given by

$$(1+\mu)x^4 + [(2\mu+3)\varepsilon^2 - 1]x^2 + \varepsilon^2(1+\mu\varepsilon^2) = 0. \tag{18}$$

If we chose the parameters to be $\varepsilon = 0.1$ and $\mu = 1$, this equation gives the coordinates of maximum and minimum of x-nullcline, as plotted in Figure 2:

$$\begin{aligned} x_{max} &= 0.105 \quad x_{min} = 0.66 \\ z_{max} &= 5.14 \quad z_{min} = 2.79. \end{aligned} \tag{19}$$

These extreme are bifurcations points, meaning that there the stability of system changes.

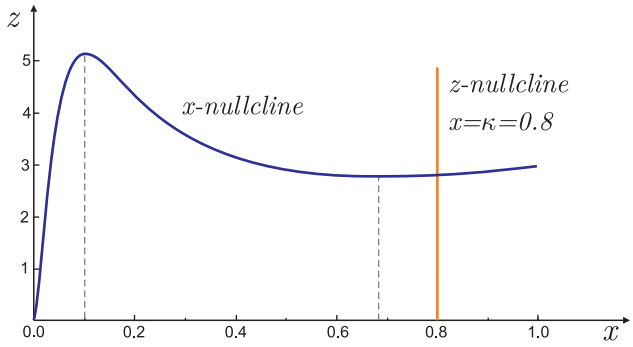

Figure 2. Phase-plane portret of nullclines given by Eqs. (16) and (17)

Let us now form the Jacobian matrix for Eqs. (11) and (12) in the steady state (Eqs. (14) and (15)):

$$\mathcal{J} = \begin{pmatrix} \frac{\partial f}{\partial x} & \frac{\partial f}{\partial z} \\ \frac{\partial g}{\partial x} & \frac{\partial g}{\partial z} \end{pmatrix} = \begin{pmatrix} \frac{2\kappa^2(1-\varepsilon^2)}{\rho_0(\varepsilon^2+\kappa^2)^2} & \mu\rho_0 \\ -1 & 0 \end{pmatrix}, \tag{20}$$

where ρ_0 is the Eq. (7) for $x = \kappa$ (in steady state).

The determinant of Jacobian matrix is by all means positive

$$\det \mathcal{J} = \mu\rho_0 > 0. \tag{21}$$

It is remarkable that the trace of matrix, Eq. (20) mainly depends on the parameter κ:

$$\mathrm{Tr}\mathcal{J} = \frac{2\kappa^2(1-\varepsilon^2)}{\rho_0(1+\kappa^2)^2} - \mu\rho_0 - 1, \tag{22}$$

or more explicitly

$$\mathrm{Tr}\mathcal{J} = \frac{-(1+\mu)\kappa^4 + (1-3\varepsilon^2-2\mu\varepsilon^2)\kappa^2 - \varepsilon^2(1+\mu\varepsilon^2)}{(1+\kappa^2)(\varepsilon^2+\kappa^2)}. \tag{23}$$

The sign of $\mathrm{Tr}\mathcal{J}$ is provided by the numerator in Eq. (23). It represents a downward open parabola represented in Figure 3.

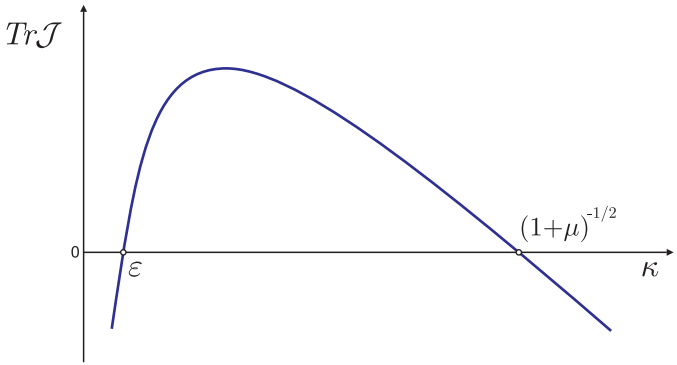

Figure 3. The plot of how the sign of $\mathrm{Tr}\mathcal{J}$ depends on parameter κ.

For small ε,Tr$\mathcal{J}$ is positive in the interval

$$\varepsilon < \kappa < (\mu + 1)^{-1/2} \tag{24}$$

so that the eigenvalue γ for Jacobian matrix, Eq. (20), is expressed by

$$\gamma_{1/2} = \frac{1}{2}\left\{\mathrm{Tr}\mathcal{J} \pm \left[(\mathrm{Tr}\mathcal{J})^2 - 4\det\mathcal{J}\right]^{1/2}\right\}, \tag{25}$$

meaning that the steady state Eqs. (14) and (15) is unstable in the interval of Eq. (24). In that interval the considered reaction exhibits limit cycle oscillations. This regime is of interest for the case where diffusivity of reactants is taken into account, which is the subject of the next section.

3 Symmetry breaking instability in this model of autocatalytic reaction with diffusion of reactants X and Y

In the following we will consider the circumstances where parameters $(\kappa, \mu, \varepsilon_0)$ have the values to provide steady-state, Eqs. (14) and (15). Then we will examine the role of reactants diffusivity within harmonic spatial perturbation of steady-state checking if it would lead to symmetry breaking instability of the reaction elaborated in the preceding section. In the literature a commonly used reactor for the study of such chemical dynamics, is the continuous flow well-stirred tank reactor (CSTR). It is also known as backmix reactor [9]. Let us now add the diffusion terms on the right hand sides of Eqs. (5) and (6), respectively:

$$D_x\frac{\partial^2 X}{\partial \ell^2} \qquad\qquad D_y\frac{\partial^2 Y}{\partial \ell^2}, \tag{26}$$

where D_x, D_y are the corresponding constant diffusion coefficients with dimensions $\left[\mathrm{m^2 s^{-1}}\right]$. The length $\ell\,[\mathrm{m}]$ is taken along coordinate axis of "one dimensional" tube of CSTR, where the reaction with diffusion takes part.

We will then introduce the dimensionless length ξ as follows [10]:

$$\xi = \frac{\ell}{\ell_0}, \tag{27}$$

where ℓ_0 is the characteristic diffusion length for reactants. Thus, the nondimensionalized diffusion terms now read:

$$\begin{array}{ll} \mathcal{D}_x \frac{\partial^2 x}{\partial \xi^2}; & \mathcal{D}_x = \frac{D_x K_n}{\ell_0^2 K_2} \\ \mathcal{D}_y \frac{\partial^2 y}{\partial y^2}; & \mathcal{D}_y = \frac{D_y K_n}{\ell_0^2 K_2}. \end{array} \tag{28}$$

Consequently, by adding of these new terms into Eqs. (11) and (12), and introducing a suitable auxiliary variable z:

$$z = x + y, \tag{29}$$

we now have two partial differential equations as follows:

$$\frac{dx}{d\tau} = \mu(z - x)\left(\frac{\varepsilon^2 + x^2}{1 + x^2}\right) - x + \mathcal{D}x\frac{\partial^2 x}{\partial \xi^2}, \tag{30}$$

$$\frac{dz}{d\tau} = \kappa - x + \mathcal{D}_y \frac{\partial^2 z}{\partial \xi^2} - \mathcal{D}_y \frac{\partial^2 x}{\partial \xi^2}, \tag{31}$$

We will now analyze stability properties of Eqs. (30) and (31) by considering effects of small perturbations. One should look at spatially nonuniform perturbations and estimate whether these are amplified or attenuated. If an amplification occurs, then a concentration of reactant close to the spatially uniform steady-state will be destabilized leading to some new state in which spatial variations prevail. Starting close to the homogeneous steady-state $(x_0;\ z_0)$ in Eqs. (14) and (15) we take small inhomogeneous perturbations (δ_x and δ_z) as follows:

$$x = x_0 + \delta_x \qquad\qquad z = z_0 + \delta_z, \tag{32}$$

where pertaining inequalities safely holds:

$$\frac{\delta x}{x_0} \ll 1 \qquad\qquad \frac{\delta z}{z_0} \ll 1. \tag{33}$$

When reactant solution is well mixed, it is plausible that we rely on the fact that x_0 and z_0 are constant in time and spatially uniform (independent of τ and ξ), so it yields:

$$\begin{array}{ll} \frac{\partial}{\partial\tau}(x_0+\delta x)=\frac{\partial\delta x}{\partial\tau} & \frac{\partial}{\partial\tau}(z_0+\delta z)=\frac{\partial\delta z}{\partial\tau} \\ \frac{\partial^2}{\partial\xi^2}(x_0+\delta x)=\frac{\partial^2\delta x}{\partial\xi^2} & \frac{\partial^2}{\partial\xi^2}(z_0+\delta z)=\frac{\partial^2\delta z}{\partial\xi^2}. \end{array} \tag{34}$$

Inserting the expressions from Eqs. (32) into the system of Eqs. (30) and (31) and relying on (x_0, z_0) from Eqs. (14) and (15) we arrive at the new format of this system

$$\frac{\partial\delta x}{\partial\tau}=\left(\frac{2\kappa^2(1-\varepsilon^2)}{\rho_0(1+\kappa^2)^2}-\mu\rho_0-1\right)\delta x+\mathcal{D}_x\frac{\partial^2 x}{\partial\xi^2}+\mu\rho_0\delta z, \tag{35}$$

$$\frac{\partial\delta z}{\partial\tau}=-\delta x-\mathcal{D}_y\frac{\partial^2 x}{\partial\xi^2}+\mathcal{D}_y\frac{\partial^2 z}{\partial\xi^2}. \tag{36}$$

Note that in the derivation of Eqs. (35) and (36) we discarded small terms of quadratic order of type δx^2, $\delta x\delta z$, preserving just linear form of small perturbations [10].

We shall build solutions to Eqs. (35) and (36) from the basic functions $\exp(\sigma\tau)$ and $\cos(q\xi)$, where σ is the growth rate of perturbation and q is the dimensionless wave number. It is appropriate that we restrict our attention to the following trial option [10]: by separation of variables (τ, ξ), as follows

$$\delta x=A\cdot f(\tau,\xi); \qquad \delta z=B\cdot f(\tau,\xi); \qquad f(\tau,\xi)=\exp(\sigma\tau)\cos(q\xi), \tag{37}$$

where A and B are respective small amplitudes of perturbations of initial time $\tau=0$ $(t=0)$.

The exponential time dependence $\exp(\sigma\tau)$ would be suitable for either increasing $(\sigma>0)$ or decreasing $(\sigma<0)$ perturbation. We need to determine if $\sigma>0$, thus providing that the symmetry-breaking instability of the uniform steady-state is compatible with the model considered here. In realistic circumstances δ_x and δ_z might have more complicated spatial forms. Then the Fourier theorem states that such a form of perturbation can be expressed as an infinite sum of terms of type $\cos(nq\xi)$, where

$n = 1, 2, 3, ...$ with decreasing amplitudes. For the sake of simplicity, we are merely taking only leading component, Eq. (37) which could be considered a dominant mode in Fourier expansion. It is apparent that from expressions in Eq. (37) easily follows the set of auxiliary equations:

$$\frac{\partial \delta x}{\partial \tau} = A\sigma \cdot f(\tau, \xi) \qquad \frac{\partial \delta z}{\partial \tau} = B\sigma \cdot f(\tau, \xi) \tag{38}$$

$$\frac{\partial^2 \delta x}{\partial \xi^2} = -Aq^2 \cdot f(\tau, \xi) \qquad \frac{\partial^2 \delta z}{\partial \xi^2} = -Bq^2 \cdot f(\tau, \xi) \tag{39}$$

Inserting Eqs. (37), (38) and (39) in the system of Eqs. (35) and (36), we safely get (by cancelling the common factor $f(\tau, \xi)$ the system of algebraic homogeneous equations for unknown amplitudes A and B:

$$\begin{gathered} \left(\sigma + \mu\rho_0 + \mathcal{D}_x q^2 + 1 - \frac{2\kappa^2(1-\xi^2)}{\rho_0(1+\kappa^2)^2}\right) A - \mu\rho_0 B = 0, \\ (1 - \mathcal{D}_y q^2)A + (\sigma + \mathcal{D}_y q^2)B = 0. \end{gathered} \tag{40}$$

To get nonzero perturbations it is needed to have $A \neq 0$ and $B \neq 0$. The only way this can be achieved is by setting the determinant of Eq. (40) equal to zero

$$\det \begin{pmatrix} \sigma + 1 + \mu\rho_0 - \varphi + \mathcal{D}_x q^2 & -\mu\rho_0 \\ 1 - \mathcal{D}_y q^2 & \sigma + \mathcal{D}_y q^2 \end{pmatrix} = 0, \tag{41}$$

where we used the abbreviation

$$\varphi = \frac{2\kappa^2(1-\varepsilon^2)}{\rho_0(1+\kappa^2)^2}. \tag{42}$$

This parameter will play a crucial role in forthcoming calculations. If we put Eq. (41) in the more compact version

$$\det \begin{pmatrix} m_{11} + \sigma + \mathcal{D}_x q^2 & m_{12} \\ m_{21} - \mathcal{D}_y q^2 & \sigma + \mathcal{D}_y q^2 \end{pmatrix} = 0, \tag{43}$$

we see that $m_{11} = 1 + \rho\mu_0 - \phi$, $m_{12} = -\rho\mu_0$, $m_{21} = 1$ and $m_{22} = 0$ are exactly the matrix elements of Jacobian matrix (Eq. (20)), where diffusivities of X and Y are missing. Expanding determinant in Eq. (41)

and by grouping the terms of the polynomial with respect to σ, we get

$$\begin{array}{c} \sigma^2 + \left[(\mathcal{D}x + \mathcal{D}_y)q^2 + 1 + \rho_0\mu - \varphi\right]\sigma + \\ +\mathcal{D}_x\mathcal{D}_y q^4 + \mathcal{D}_y(1-\varphi)q^2 + \mu\rho_0 = 0 \end{array} . \tag{44}$$

This quadratic equation can be reduced to standard form

$$\sigma^2 + H\sigma + F = 0, \tag{45}$$

with corresponding abbreviations:

$$H = (\mathcal{D}_x + \mathcal{D}_y)q^2 + 1 + \rho_0\mu - \varphi, \tag{46}$$

$$F(\theta) = c\theta^2 + d\cdot\theta + e; \qquad \theta = q^2 \tag{47}$$

$$c = \mathcal{D}_x\mathcal{D}_y; \qquad d = \mathcal{D}_y(1-\varphi)\theta; \qquad e = \mu\rho_0. \tag{48}$$

First we recall that two possible roots of Eq. (45) are

$$\sigma_{1/2} = \frac{1}{2}\left(-H \pm \sqrt{H^2 - 4F}\right). \tag{49}$$

It is plausible that for the realistic values $\mathcal{D}_x$ and $\mathcal{D}_y$ and big enough q (small wavelength of perturbation, parameter H in Eq. (43) should safely be positive. But positive H implicates that there is still possible root in Eq. (49) whose real part can be negative.

In order for second root to have a positive real part, it is necessary that the value of $F(\theta)$, given by Eqs. (47) and (49) be negative. Since $F(\theta)$ is a parabola opening upwards that has a minimum, it is necessary that this minimum has negative velue, see Figure 4.

Since coefficients c and e in Eq. (47) are positive, we need that remaining coefficient d by θ should be negative

$$d = \mathcal{D}_y(1-\varphi) < 0, \tag{50}$$

which implies

$$\varphi = \frac{2\kappa^2(1-\varepsilon^2)}{\rho_0(1+\kappa^2)^2} > 1. \tag{51}$$

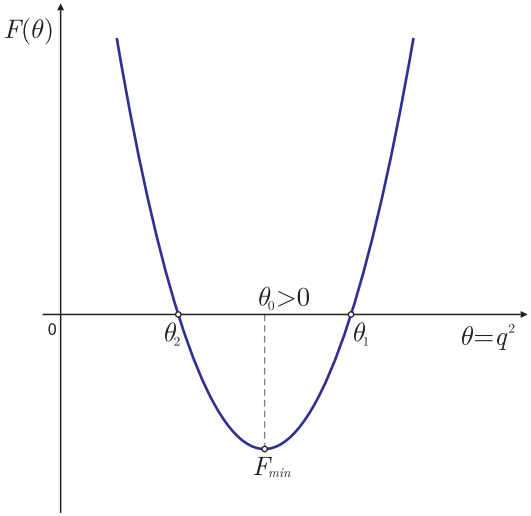

Figure 4. A schematic representation of necessary conditions for negative $F(\theta)$.

In order to complete the necessary and sufficient condition for the negative minimum of $F(\theta)$ from Eq. (47) we take the derivative

$$\frac{dF}{d\theta} = 2c\theta + d = 0 \qquad \Rightarrow \qquad \theta_0 = -\frac{d}{2c}. \tag{52}$$

On the basis of Eqs. (47), (48) and (49), we get

$$\theta_0 = \frac{\varphi - 1}{2\mathcal{D}_x} > 0. \tag{53}$$

Inserting θ_0 in Eqs. (47) and (48), the minimum of $F(\theta)$ reads

$$F_{min} = -\frac{1}{4}\frac{\mathcal{D}_y}{\mathcal{D}_x}(\varphi - 1)^2 + \rho_0\mu. \tag{54}$$

Now we impose that F_{min} in Eq. (54) should be negative, which implies

$$(\varphi - 1)^2 > 4\rho_0\mu\frac{\mathcal{D}_x}{\mathcal{D}_y}, \tag{55}$$

or otherwise

$$\frac{\mathcal{D}_y}{\mathcal{D}_x} > \frac{4\rho_0\mu}{\left(\frac{2\kappa^2(1-\varepsilon^2)}{\rho_0(1+\kappa^2)^2}-1\right)^2}. \tag{56}$$

In order to estimate the ratio of diffusion coefficients according to Eq. (56), the reasoning could be as follows: we chose small parameter ε to be

$$\varepsilon = 0.1 \qquad \Rightarrow \qquad \varepsilon^2 = 0.01. \tag{57}$$

Regarding the parameter μ we assume $\nu < K_1$, so we take

$$\mu = 0.5. \tag{58}$$

Recalling Eq. (24), we here have

$$0.1 < \kappa < \frac{1}{\sqrt{1+0.5}} \qquad \Rightarrow \qquad 0.1 < \kappa < 0.81. \tag{59}$$

If we choose $\chi = \kappa = 0.7$ (ρ_0 from Eq. (7)), and calculate the auxiliary paramters as follows

$$\rho_0 = \frac{0.01 + 0.49}{1 + 0.49} = 0.3356, \tag{60}$$

and

$$\varphi = \frac{2 \cdot 0.49 \cdot (1 - 0.01)}{0.3356 \cdot (0.49 + 1)^2} = 1.3, \tag{61}$$

inserting Eqs. (58), (60) and (61) into inequality Eq. (56), we finally get

$$\frac{\mathcal{D}_y}{\mathcal{D}_x} \geq 7.46. \tag{62}$$

This number meets the requirement from Eq. (3), meaning that remarkable difference in diffusivities should be provided in order to get inhomogeneous spatial distribution of reactants, slow diffusive X and fast diffusive substrate Y. This could be possible if the reaction product X molecules are associated to some appropriate slowly diffusing buffer.

We recall CIMA reaction in Introduction, where it was achieved in a way that the activator reactant triiodide is transiently complexed with

starch molecule and thus its effective diffusion is reduced remarkably in comparison with free diffusion [3,10]. We could now estimate the values of wavenumber q for crossing points θ_1 and θ_2 of parabola plotted in Figure 4. These are the solutions of $F(\theta) = 0$, from Eqs. (47) and (48), which gives

$$\theta_{1/2} = \frac{1}{2\mathcal{D}_x\mathcal{D}_y}\left[\mathcal{D}_y(\varphi-1) \pm \sqrt{\mathcal{D}_y^2(\varphi-1)^2 - 4\mathcal{D}_x\mathcal{D}_y\mu\rho_0}\right]. \tag{63}$$

In order to get positive real numbers it is necessary to be fulfilled the inequality

$$\mathcal{D}_y^2(\varphi-1)^2 - 4\mathcal{D}_x\mathcal{D}_y\mu\rho_0 > 0. \tag{64}$$

This is the same condition expressed in Eq. (55). If we use the following set of parameters:

$$\mu = 0.5 \qquad \varphi = 1.3 \qquad \rho_0 = 0.3356 \qquad \mathcal{D}_x = 0.1 \qquad \mathcal{D}_y = 1, \tag{65}$$

we get the respective wavenumbers:

$$\theta_1 = 2.25 \quad \text{or} \quad (q_1 = 1.5) \qquad \theta_2 = 0.75 \quad \text{or} \quad (q_2 = 0.87). \tag{66}$$

Taking into account that the dimensionless q is expressed in terms of dimensionless wavelength $\Lambda = \lambda/\ell_0$, as follows

$$q = \frac{2\pi}{\Lambda} = \frac{2\pi}{\lambda}\ell_0, \tag{67}$$

so we get dimensionless wavelength

$$\lambda = \frac{2\pi}{q}\ell_0. \tag{68}$$

On the basis of numerical values in Eq. (66) it gives pretty narrow domain

$$\lambda_1 = 4.2\ell_0 \qquad\qquad \lambda_2 = 7.2\ell_0. \tag{69}$$

If we choose $\lambda = 6\ell_0$, and impose zero boundary condition for gradient of perturbative concentration at the positions $\ell = 0$, and $\ell = L$ (where 0 and

L are the end points of CSTR reactor), we have

$$\left| -\frac{\partial}{\partial \xi}(\cos q\xi) \right| = \sin q\xi = 0 \qquad \Rightarrow \qquad q\xi = n\pi \qquad n = 1, 2, 3, ... \quad (70)$$

or in dimensionless form ($\lambda = 6\ell_0$)

$$\frac{2\pi}{\lambda}\ell_0 \frac{L}{\ell_0} = n\pi \qquad L = 3\ell_0 n. \quad (71)$$

This is plotted in Figure 5, for reactant X. The above could permit us the

Figure 5. The one-dimensional space distribution of reactant activator $x = x_0 + A\cos(q\xi)$ for the mode with $\lambda = 6\ell_0$, where $\ell_0 = \sqrt{Dt}$ is the characteristic diffusion length. $x_0 = \kappa = 0.7$, $A = 0.05$, $L = 3\ell_0 n$. The amplitude is exaggerated in order to be easily noticeable. The dot line is the steady-state level of the concentration of X.

following interpretation of how diffusive instability is caused as a result of random perturbations; a small peak concentration of substrate Y creates increased concentration of product X. But this result, along with fast diffusion of Y, brings about substrate depletion thus preventing unlimited growth peak of X. This is important since our analysis works only as long as the perturbations are sufficiently small to render the linear approximations of Eqs. (32) and (33) are valid picture of nonlinear system of Eqs. (30) and (31). If perturbation is beyond small size, this analysis would be inadequate.

4 Conclusion

In this paper we are focused on specific positive feedback (or substrate depletion) reaction-diffusion autocatalytic system. It consists of substrate Y and the product X autocatalyzed in terms of allosteric catalyzer. Under suitable conditions related to the values of pertaining diffusion coefficients and reaction rates of X and Y the small perturbation of their concentrations can lead to symmetry-breaking instability which yields heterogeneous spatial patterns. We intuitively associate diffusion with a smoothing and homogenizing influence that eliminates chemical gradients leading to uniform spatial distribution. Instead, here it appears that different diffusion reactants act positively, engendering gradients and fostering nonuniform pattern-like forms of reactant concentrations. We have proven that the diffusion constants of substrate Y versus activator X should be remarkably different ($D_y/D_x \sim 7.4$) in order to meet the restrictive conditions for symmetry-breaking instability. We suggest that lowering diffusivity of product X can be achieved by proper buffer with low diffusivity. We recall that such role in successful experiment was achieved by starch molecules (CIMA reactions [3, 7]).

***Acknowledgment*:** This work is supported by Serbian Academy of Sciences and Arts, personal grant No. Φ134.

References

[1] A. Goldbeter, Dissipative structures and biological rhythms, *Chaos* **27** (2017) #104612.

[2] A. Goldbeter, Dissipative structures in biological systems; bistability, oscillations, spatial patterns and waves, *Phil. Trans. R. Soc. A* **376** (2018) #20170376.

[3] A. Hanna, A. Saul, K. Showalter, Detailed studies of propagating fronts in the iodate oxidation of arsenous acid, *Am. Chem. Soc.* **104** (1982) 3838–3844.

[4] A. M. Turing, The chemical basis of morphogenesis, *Phil. Trans. R. Soc. B* **237** (1952) 37–72.

[5] G. Nicolis, I. Prigogine, Self-organizing in nonequilibrium systems, from dissipative structures to order through fluctuations, Wiley, New York, 1977.

[6] I. Prigogine, R. Lefever, Symmetry breaking instabilities in dissipative systems. II, *J. Chem. Phys.* **48** (1968) 1695–1700.

[7] I. R. Epstein, K. Showalter, Nonlinear Chemical Dynamics: Oscillations, Patterns, and Chaos, *J. Phys. Chem.* **100** (1996) 13132–13147

[8] J. J. Tyson, Biochemical oscillators, in: C. P. Fall, E. S. Marland, J. M. Wagner, J. J. Tyson (Eds.), *Computational Cell Biology*, Springer, New York, 2002, pp. 230–260.

[9] M. Choplin, C. Bucke, *Enzyme Technology*, Univ. Press, Cambridge, 1990.

[10] M. V. Satarić, T. Nemeš, J. A. Tuszynski, Re-examination of the Sel'kov model of glycolysis and its symmetry-breaking instability due to the impact of diffusion with implications for cancer imitation caused by Warburg effect, *Biophysica* **4** (2024) 545–560.

[11] S. N. Semenov, L. J. Kraft, A. Ainla, M. Zhao, M. Baghbanzadeh, V. E. Campbell, K. Kang, J. M. Fox, G. M. Whitesides, Autocatalytic, bistable, oscillatory networks of biologically relevant organic reactions, *Nature* **537** (2016) 656–660.